



Controlled Micelle Formation and Stable Capture of Hydrophobic Drug by Alkylated POSS Methacrylate Block Copolymers

Chatterjee, Suchismita
Ohshio, Maho
Yusa, Shin-ichi
Ooya, Tooru

(Citation)

ACS Applied Polymer Materials, 1(8):2108-2119

(Issue Date)

2019-07-11

(Resource Type)

journal article

(Version)

Accepted Manuscript

(Rights)

© 2019 American Chemical Society

(URL)

<https://hdl.handle.net/20.500.14094/90008022>



Controlled Micelle Formation and Stable Capture of Hydrophobic Drug by Alkylated POSS Methacrylate Block Copolymers

Suchismita Chatterjee¹, Maho Ohshio², Shin-ichi Yusa², Tooru Ooya^{1}*

¹Graduate School of Engineering, Department of Chemical Science and Engineering, Kobe
University, 1-1 Rokkodai-cho, Nada-Ku, Kobe 657 8501, Japan

²Graduate School of Engineering, University of Hyogo, 2167 Shosha, Himeji, Hyogo 671-
2280, Japan

*E-mail: ooya@tiger.kobe-u.ac.jp

Abstract

Design of polymeric micelles, formed by self-assembly of amphiphilic block copolymers, is crucial for encapsulation of poorly soluble drugs leading to the development of promising carrier systems. Herein, we synthesized amphiphilic di-block copolymers of 2-(methacryloyloxy)ethyl phosphorylcholine (MPC) and methacrylate R-polyhedral oligomeric silsesquioxanes (POSS) (vertex R-groups of POSS cage modified with ethyl (C_2H_5), hexyl (C_6H_{13}), octyl (C_8H_{17}) alkyl chain) via RAFT polymerization technique. Polymeric micelle was formed in aqueous environment, and the absolute size was calculated to be around 26-43 nm. The increased alkyl chain of the R-groups of POSS led to loosely packed association of the micelles. The polymeric micelles encapsulated the hydrophobic model drugs (paclitaxel and α -tocopherol), and the encapsulation efficiency was strongly dependent on the structure of drug molecules. The drug-loaded micelles were stable for 5 days at 25 °C. The release % of both the drugs from the micelles was negligible level or below 20%, suggesting the strong interaction between the R-POSS moieties and the drug molecules. Cellular uptake of the micelles by HeLa cells were quantitatively analyzed using a FITC-labelled paclitaxel (FITC-PTX). All the micelles were internalized by the cell after 2 h, and cellular uptake of PTX-loaded micelle composed of the C_6H_{13} -POSS copolymer reached to the highest level, suggesting that alkyl chain length is one of the tunable factors for the cellular uptake. These di-block copolymers have great potential as hydrophobic drug carrier molecule and its delivery to specific sites.

Keywords

2-methacryloyloxyethyl phosphorylcholine; polyhedral oligomeric silsesquioxanes; RAFT polymerization; micelles; hydrophobic drug carrier; cellular uptake

1. Introduction

Nanoparticle-mediated drug delivery has shown tremendous progress in cancer therapy, where the side effects of chemotherapeutic drugs are reduced by nanoparticle invasion into tumour sites. Controlling the appropriate size of nanoparticles is important to deliver the poorly soluble drugs to the tumor tissues via the passive enhanced permeability with negligible biotoxicity to other organs. Also, the nanoparticles have to escape the macrophage phagocytosis and the rapid clearance from blood circulation. The nanometric micelles, which is one of the nanoparticle systems formed by self-assembly of amphiphilic polymers, have been studied extensively for their functionality in the enhancement of the solubility of poorly soluble drugs. The polymeric micelles consist of a lipophilic core that solubilizes hydrophobic drugs and a hydrophilic shell that makes the entire micelle system water-soluble. Small dimensions of polymeric micelles (< 200 nm) avoid recognition of the reticular endothelial system (RES)^{1,2}.

In order to control the size of polymeric micelles, the controlled radical polymerization of amphiphilic di-block copolymers composed of a hydrophilic and hydrophobic segments has been extensively studied for biomedical applications³⁻⁶. Especially, reversible addition–fragmentation chain transfer (RAFT) polymerization⁷⁻¹⁰ is known as the representative method to prepare amphiphilic block copolymers for biomedical applications¹¹. The representative hydrophilic chain of the di-block copolymers is poly(ethylene glycol) (PEG), which can be easily utilized as a chain transfer agent to prepare a di-block copolymer with *tert*-butyl 2-((4-hydroxybutanoyloxy)methyl)acrylate¹². Alternatively, 2-methacryloyloxyethyl phosphorylcholine (MPC) has been subjected to the RAFT polymerization. For example, Strnzel et al. reported the development of an amphiphilic block copolymer through RAFT polymerization of a phosphorylcholine-based acrylate and butyl acrylate¹³. Yusa et al. also

reported the synthesis of well-defined amphiphilic copolymers through RAFT polymerization of MPC and *n*-butyl methacrylate (BMA), which formed polymeric micelles bearing good solubilization property of paclitaxel (PTX)¹⁴. As a result, a copolymer of MPC with hydrophobic units possesses excellent biocompatibility for biomedical applications. The amphiphilic di-block copolymers composed of poly(MPC) chain have been also studied for pH-responsive system and nanoparticles as a drug carrier and a diagnostic reagent¹⁵. The advantage of the MPC-based polymeric micelles includes the enhanced cellular uptake comparing with the PEG-based polymeric micelles. A copolymer of poly(MPC)-*b*-poly[2-(diisopropyl-amino)ethyl methacrylate] (PDPA) formed a micelle, and the assembly was incorporated into cancer (HeLa) cell with much higher degree as compared to normal cells, mainly due to the stronger binding of PMPC to cell membranes^{16, 17, 18}.

The choice of the hydrophobic part of the amphiphilic di-block copolymers is thought to be an important factor to stabilize the micelle systems. The polyhedral oligosilsesquioxane (POSS) bears nanostructures consisting of both organic and inorganic matter with an inner core of inorganic silicon and oxygen and an outer layer of organic constituents¹⁹. POSS enhances the mechanical and thermal properties of polymers through physical mixing which depends on the state of the POSS dispersion, the surface functional group of POSS, amount of POSS, crystallinity, morphology, and so on¹⁹.

Based on the physicochemical properties of POSS, a methacrylate POSS as a hydrophobic monomer has been studied to prepare block copolymers. For example, Hussain et al. have reported for the first time that tailored formation of block copolymers consisting of poly(ethylene glycol) (PEG) and poly(methacrylisobutyl polyhedral oligomeric silsesquioxane) P(MA-POSS) as the hydrophilic and hydrophobic blocks, respectively^{20, 21}. The P(MA-POSS) in the di-block copolymer acted as a hydrophobic core of the polymeric micelles with 0.1 mg/ml of CMC: Strong hydrophobicity of POSS block and its ability to self-assemble into

micelles at relatively lower block copolymer concentrations, which might be advantageous in comparison with the other alkyl methacrylate-based block²¹. Zhang et al. prepared a polymerizable monomer of POSS that was conjugated with 2-hydroxyethyl methacrylate, and the monomer (PHEMAPOSS) was used for preparing PHEMAPOSS-block copolymer via the RAFT polymerization²². Most recently, POSS-based zwitterionic polymer has been focused on nanoparticle formation and encapsulation of doxorubicin: supramolecular complexation in combination with cyclodextrin-adamantane inclusion complex led to stable nanoparticle formation with effective cellular uptake²³. The POSS has also been utilized as a strong hydrophobic core of a unimolecular micelle²⁴ and nanostructured core-shell nanoparticles²⁵ for controlled release of anticancer drugs. Thus, POSS with inert vertex groups on the silicon-oxygen cage (hydrophobic in nature) promotes the formation of a well-patterned micelle structure and controls the release of the drug. In our previous studies, investigation on copolymer developed through random polymerization of methacrylate POSS bearing different alkyl vertex groups as a hydrophobic monomer and MPC as hydrophilic monomer was performed. The POSS moieties enhanced the hydrophobicity of the copolymer at water-polymer interface²⁶, enhanced the solubility of PTX in aqueous environment²⁷ and enhanced the dissolution of PTX from solid formulation²⁸. However, since the sequence of the POSS methacrylate and MPC cannot be controlled when using random polymerization technique, so subsequently there was no control to achieve a desired size of polymeric micelles.

In this study, the di-block copolymers of the POSS methacrylate and MPC were synthesized by RAFT polymerization. The effect of the alkyl chain length of the vertex R-groups [ethyl (C₂H₅), hexyl (C₆H₁₃), octyl (C₈H₁₇)] of POSS methacrylate on the size and morphology of the polymeric micelle formation has been discussed. The encapsulation and releasing behavior of paclitaxel (PTX) and α -tocopherol (α -TP) was studied to understand the interaction between the chemical structure of the hydrophobic drug and the hydrophobic domain (POSS cage

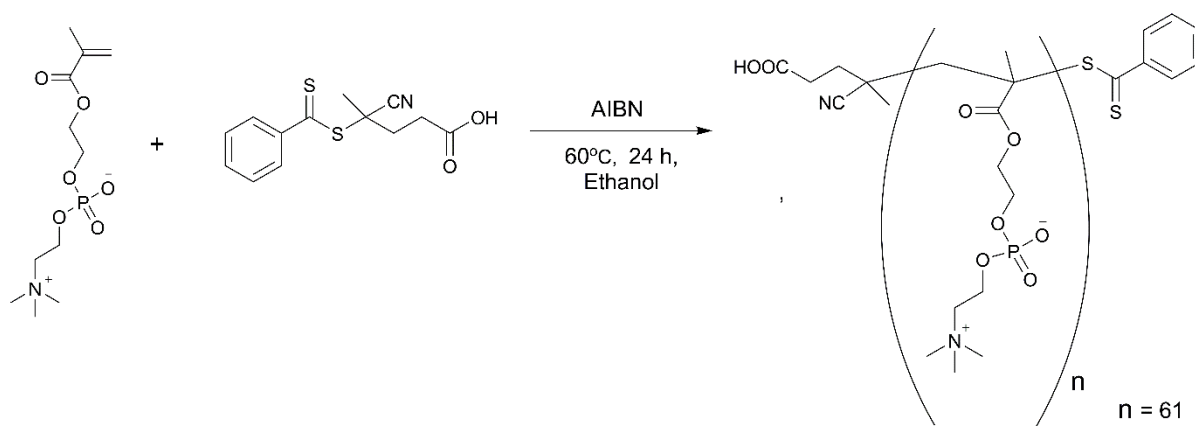
bearing different vertex R-group) of copolymers. The cellular uptake of copolymer micelle was investigated by FITC-labelled PTX-loaded polymeric micelle in HeLa cell line using fluorescence microscopy and flow cytometry analysis. The correlation between the vertex R-group of POSS, the size of the micelle, and cellular uptake were evaluated from the dynamic light scattering (DLS) measurements, fluorescence microscopy and flow cytometric measurements, and the effect of the R-groups of the POSS methacrylate in the di-block copolymers on the hydrophobic drug delivery has been discussed.

2. Materials and Methods

2.1 Materials

2-(Methacryloyloxy) ethyl phosphorylcholine (MPC) was kindly supplied by Prof. Kazuhiko Ishihara (University of Tokyo, Japan). AIBN was purified by recrystallization from methanol before use. Ethyltrimethoxysilane, hexyltrimethoxysilane, and trimethoxyoctylsilane were purchased from Tokyo Chemical Industry Co. Inc, (Tokyo Japan.). The 3-methacryloxypropyl trichlorosilane was purchased from Sigma-Aldrich (Tokyo, Japan). Dulbecco's Modified Eagle Medium (DMEM), Dulbecco's phosphate-buffered saline (D-PBS), 0.25 %-Trypsin/1mM-EDTA solution, penicillin-streptomycin mixed solution and sodium carbonate were purchased from Nacalai Tesque, Inc. (Kyoto, Japan). Fetal Bovine Serum (FBS) was purchased from Sigma-Aldrich Co. LLC. (St. Louis, U.S.A). Water used in all experiment was purified with Millipore Milli-Q system. The other reagents and solvents were used without any further purification. HeLa cells (Health Science Research Resources Bank, Osaka, Japan) were cultured in DMEM supplemented with 10% FBS and 100 U/mL penicillin-streptomycin mixed solutions. Cells were grown in a humidified incubator at 37 °C under 5% CO₂.

2.2 Preparation of poly(2-(methacryloyloxy)ethyl phosphorylcholine)-based chain transfer agent (PMPC₆₁) (Scheme 1)



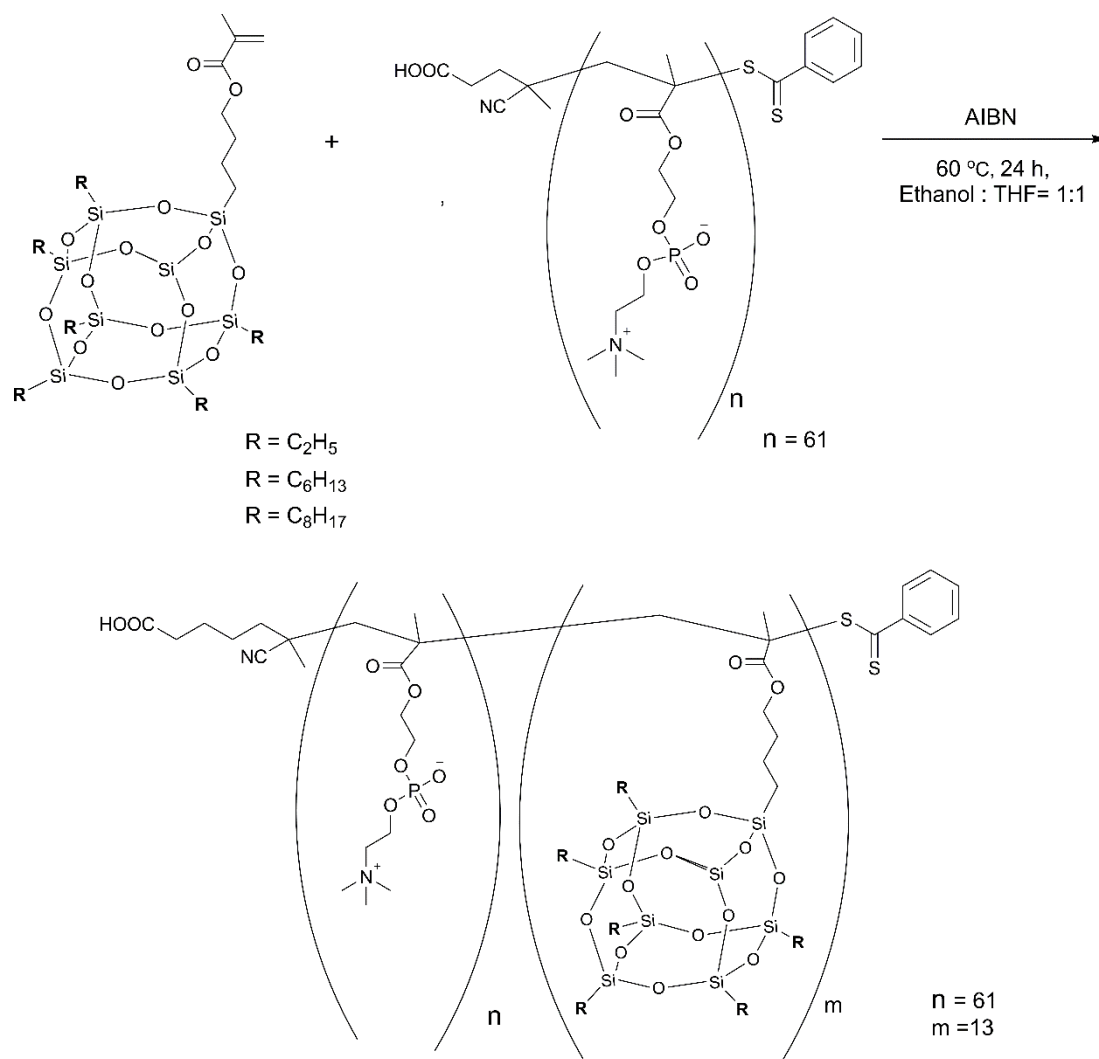
Scheme 1: Synthesis of poly(2-(methacryloyloxy)ethyl phosphorylcholine)-based chain transfer agent (PMPC₆₁)

MPC (10 mmol, 2.95 g) was dissolved in dry ethanol (10 ml). Cyanopentanoic acid dithiobenzoate (CPD) (0.2 mmol, 0.0559 g), AIBN (0.05 mmol, 82 mg) were added to the solution. The mixed solution was deoxygenated by purging N₂ gas for 30 min. It was then transferred to the polymerization chamber with temperature set at 60 °C and put under continuous stirring process for 24 h. After cooling, the solution was dialyzed against deionized water for 3 days. The obtained PMPC macro-CTA (PMPC₆₁) was recovered by freeze-drying. The number-average molecular weight (M_n =18,275) and degree of polymerization (DP = 61) of PMPC₆₁ was determined by ¹H NMR spectra, in which the peaks at 7.3-7.9 ppm (phenyl, 5H) and 3.7 ppm (N-CH₂,2H) were subjected for the integration.

2.3 Preparation of R-POSS-based MPC di-block copolymers (Scheme 2)

PMPC₆₁ (182.8 mg), C₂H₅-POSS MA (224 mg, 0.3 mmol), C₆H₁₃-POSS MA (316 mg, 0.3 mmol) and C₈H₁₇-POSS MA (401 mg, 0.3 mmol) and AIBN (0.33 mg, 0.002 mmol) were dissolved in ethanol and THF mixture (volume ratio: 1:1, 3ml). The solution was degassed and

filled with N₂ by five freeze-pump-thaw cycles. The polymerization was carried out at 60 °C for 24 h. The reaction mixture was poured into an excess amount of diethyl ether to precipitate the polymer. The polymer was purified by precipitating it two times from methanol into large amount of diethyl ether.



Scheme 2: Synthesis of R-POSS-based MPC di-block copolymers

2.4 Measurements

¹H NMR spectra were measured by dissolving copolymers in a mixture of methanol-*d*₃ : tetrahydrofuran-*d*₈ (50:50) at a concentration of 3 mg/ml using a JEOL JNM-ECZS400FT NMR System. Fourier transform infrared (FTIR) spectra were recorded on a FTIR spectrophotometer (JASCO FT/IR-460plus, Tokyo, Japan). The scanning wave numbers

ranged from 4,000 to 400 cm^{-1} . The spectrum resolution was 4 cm^{-1} , and the scans at a rate of 2 mm/sec were accumulated to determine one spectrum. Dynamic light scattering (DLS) and ζ -potential measurements were carried out using a light scattering instrument (Zetasizer Nano ZS, Malvern Instrument Ltd. Co., Worcestershire, UK). The measurements were performed at 25 °C in a 10 mM PBS (pH 7.4) with the copolymer concentration of 0.5 or 1 mg/ml. Samples were filtered by 0.45 μm pore size filter before measurements. The critical association concentration (CAC) was measured using DLS to the aqueous polymer solution of concentration varying from 0.0001 to 1 mg/ml. Above the CAC, the intensity of scattering light increases due to the presence of micelles and the intercepts obtained in the correlation functions are much higher. HPLC measurements were performed by using a GILSON HPLC system (UV-vis detector : Gilson 119 UV/VIS Detector, GILSON, Middleton, WI, U.S.A. Pump : GILSON 805 Manometric Module, GILSON 811c dynamic mixer and GILSON 306 Pump, GILSON, Middleton, WI, U.S.A., Injector : GILSON DILTOR401, GILSON, Middleton, WI, U.S.A.) with a TSKgel ODS-100S (Φ 4.6 mm \times 150 mm) (TOSOH Co., Japan) as stationary phase at room temperature. Transmission electron microscopy (TEM) images were collected using a TEM apparatus (JEOL JEM-1230, JEOL, Japan) at an accelerating voltage of 100 kV. Samples were prepared on 200 mesh copper grids. Before the measurements, the samples were vacuum dried and kept overnight *in vacuo*.

Static light scattering (SLS) measurements were performed using Otsuka Electronic Photol (Osaka, Japan) DLS-7000 at 20 °C. A He–Ne laser (10.0 mW at 632.8 nm) was used as a light source. Each copolymer was dissolved in a 10 mM PBS (pH 7.4) with polymer concentration (C_p) = 0.5 g/L and stirred overnight and then filtered using a membrane filter of 0.45 μm pore size. C₂H₅-POSS-MA-block-MPC copolymer was stirred overnight at 60 °C, but it wasn't soluble completely. The difference between the Rayleigh ratio of the solution and that of the

solvent (R_θ) due to the angular dependence can lead to the estimation of the weight-average molecular weight (M_w) and z-average radius of gyration (R_g) from the following relationship:

$$\frac{KC_p}{R_\theta} = \frac{1}{M_w} \left(1 + \frac{1}{3} R_g^2 q^2 \right)$$

where K is the optical constant and q is the magnitude of the scattering vector. The K value was calculated using $K = 4\pi^2 n^2 (dn/dC_p)^2 / N_A \lambda^4$, where n is the reflective index of the solvent, dn/dC_p is the refractive index increment against C_p , N_A is Avogadro's number, and λ is the wavelength of the light source. The q value was calculated using $q = (4\pi n / \lambda) \sin(\theta/2)$, where θ is the scattering angle. Values of dn/dC_p at 633 nm were determined using an Otsuka Electronics Photol DRM-3000 at 20 °C.

2.5 Preparation of micelles and drug-loaded micelles

Polymeric micelles were prepared by dialysis approach. Each copolymer (10 mg) was dissolved in 1 ml of ethanol with ultra-sonication for 30 min. The solutions were then added drop by drop into 10 ml of deionized water and put under vigorous stirring for 24 h. The mixture was then transferred into a dialysis tube (MWCO = 2,000) and dialyzed against water for 24 h to eliminate organic solvent. The inside phase of dialysis tube was filtered by filter with a pore size of 0.45 μm . The obtained solutions were then used for stability study by DLS and ζ -potential measurements (0, 5, 8, 11, and 12 days keeping at 25 °C).

PTX and α -TP-loaded polymeric micelles were prepared by the above-mentioned method. The copolymer to drug ratio was fixed as 10:1, which is considered to be the first choice of the drug loading. This ratio which to keep the copolymer concentration 1 mg/ml during measurements. The drug-loaded polymeric micelle solutions were then used for stability study by DLS and ζ -potential measurements (0, 2, 5 days keeping at 25 °C) and drug release study.

Amounts of PTX and α -TP loaded in the micelles were quantified by the HPLC measurements using a GILSON HPLC system (see section 2.4). The mobile phase were acetonitrile : water (60 : 40) for PTX and methanol : water (70 : 30) for α -TP, respectively. The flow rate was 1 ml/min. All the samples were dissolved in methanol, followed by filtering using filter with pore size of 0.45 μ m before the HPLC measurements. The detection was performed at a detection wavelength of 228 nm for PTX and 292 nm for α -TP. The drug loading capacity (DLC) and the drug loading efficacy (DLE) were calculated according to the following equations:

$$\text{DLC (\%)} = \frac{\text{Mass of drug in micelle}}{\text{Mass of drug loaded micelle}} \times 100 \dots (1)$$

$$\text{DLE (\%)} = \frac{\text{Mass of drug in micelle}}{\text{Mass of drug in feeding}} \times 100 \dots (2)$$

2.6 *In vitro* drug release studies

The PTX-loaded copolymer micelles (3 mg of lyophilized solid powder) were dissolved in 1 ml of D-PBS (pH 7.4). The solutions were then introduced into a dialysis membrane bag with a molecular cut-off of 6000 – 8000 Da, and they were placed in a vial containing 25 ml of mixed solution of D-PBS (pH 7.4) and 1 % Tween 80 mixed solution. The vials were placed in shaking bed maintained at the temperature of 37 °C with the shaking speed of 100 rpm. At predetermined time interval, 1 ml of the release medium was withdrawn for concentration measurement and equal volume of fresh D-PBS (pH 7.4) plus 1 % Tween 80 mixed solution was added to maintain a constant volume. One % Tween 80 maintained the sink condition and acted as solubilizing agent²⁹. The concentration of PTX released in the outer medium and PTX remaining in the PTX-loaded micelle sample after the release experiment (i.e., unreleased PTX inside dialysis tube) was monitored by the HPLC measurement (see section 2.4). The conditions of the HPLC measurements were same as described in section 2.4. All samples

were injected by 20 μ L, and the PTX was detected by UV adsorption at a detection wavelength of 228 nm. Mixture of acetonitrile (60%) and water (40%) were used as the mobile phase with flow rate of 1 ml/min. Before the measurements, the samples were filtered by filter with pore size of 0.45 μ m. *In vitro* α -TP release was also analyzed by the same procedure followed for the PTX. The conditions of the HPLC measurements were the same as described in section 2.4. To determine α -TP, a mixture of methanol and water (98:2) was used as mobile phase at a flow rate of 1.0 mL/min. All samples were injected by 20 μ l, and detection was performed at 292 nm.

2.7 Cell Viability

The cell viability of the drug-loaded polymeric micelles was determined by using Cell Counting Kit-8 (DOJINDO Laboratories, Kumamoto, Japan). HeLa cells were seeded into a 96-well plate in volumes of 90 μ l (5000 cells/ well in DMEM media supplemented with 10% FBS), and those were incubated overnight at 37 $^{\circ}$ C. Each copolymer (1 mg) was dissolved in 1 ml of D-PBS at pH 7.4 with ultra-sonication for 10 min. The drug-loaded copolymer micelles solutions (10 μ l) were added to each well to give a final concentration of PTX (2 μ g/ ml) and α -TP (108 μ g/ml) and incubated for 24 and 48 h at 37 $^{\circ}$ C. The cell viability of the copolymers without drug loading was measured following the same procedure as mentioned above, and the final concentration of the copolymers were the same as the PTX-loaded copolymer micelle concentration used in the cell viability study. As a blank (BL) and a positive control (C+), DMEM media and Hela cells without adding the copolymers were applied, respectively. A CCK-8 reagent (10 μ l) was added to each well, and it was incubated for 2 h at 37 $^{\circ}$ C. The absorbance of each well was measured using a Corona Grating Microplate Reader SH-9000 Series (Corona Electric Co., Ltd, Japan) at wavelength of 450 nm. The percentage of the viable cells was calculated using the following formula (Eq 3):

$$\% \text{ Cell Viability} = \frac{I_{450}^S - I_{450}^{BL}}{I_{450}^{C+} - I_{450}^{BL}} \times 100 \dots (3)$$

where I_{450}^S , I_{450}^{BL} and I_{450}^{C+} represent the absorbance of the samples, blank and positive control, respectively.

2.8 Cellular uptake

FITC-labelled paclitaxel (FITC-PTX) was encapsulated inside the micelles by the dialysis approach. The FITC-PTX was prepared according to the literature²⁷. HeLa Cells were seeded into a 24-well plate with a cell density of 20,000 cells/ well in 1 ml DMEM media supplemented with 10% FBS and incubated overnight at 37 °C before the experiment. After 24 h incubation, the growth media was removed and the cells were treated with serum free medium containing free FITC-PTX (2 µg/ml) and FITC-PTX-loaded micelles (equivalent FITC-PTX= 2 µg/ml) for 2 and 6 h. The media were removed and washed with D-PBS for 3 times, and each well was filled with 0.5 ml D-PBS. The cell images were immediately recorded by using a fluorescence inverted microscope (EVOS Digital Inverted Microscope, Life Technologies, Carlsbad, CA, USA).

Cellular uptake of the FITC-PTX was further quantified by flow cytometry using BD FACS Canto II flow cytometer (CA, U.S.A.). The experimental procedure was same as cellular uptake experiment except that after 2 h of incubation, the cells were collected, washed three times with D-PBS and resuspended in D-PBS for the measurement. 10,000 events were collected for each experiment and acquisitions were performed in triplicate.

3. Results and Discussion

3.1 Characterization of di-block copolymers prepared by RAFT polymerization and micelle formation

Three types di-block copolymers were prepared by RAFT polymerization by using PMPC₆₁ as the CTA, and those di-block copolymers were characterized by ¹H NMR and FT-IR measurements (section **S1, Figure S1 and S2 in Supporting Information**). The degree of polymerization of R-POSS part was calculated to be *ca.* 12-13, which was governed by the same monomer/initiator ratio. Thus, the weight ratio of PMPC and R-POSS was calculated to be 0.56 and 0.44, which was almost same ratio of PEG and poly(methacrylisobutyl polyhedral oligomericsilsesquioxane) P(MA-POSS) of PEG-P(MA-POSS) di-block copolymer (0.58 for PEG and 0.42 for P(MA-POSS))^{20,21}. Since the reported PEG-P(MA-POSS) di-block copolymer formed stable micelle in aqueous media, we chose the degree of polymerization of both PMPC and R-POSS. From the results, we determined the segment length, and the three di-block copolymers were abbreviated to MPC₆₁-*b*-C₂POSS₁₃, MPC₆₁-*b*-C₆POSS₁₃ and MPC₆₁-*b*-C₈POSS₁₂. Thus, the influence of the R-groups of POSS moiety on the micelle formation can be discussed with almost the same block length (DP of R-POSS 13/13/12). The solution properties analyzed by SLS and DLS were summarized in **Table 1**. The CAC values of all the copolymers were found in the range of 25-92 µg/ml, so that the SLS and DLS measurements of the copolymers were conducted at a concentration of 0.5 mg/ml. Since the chemical structure of the copolymers are di-block copolymers, the copolymer above the CAC concentration range are likely to form a core-shell type micelle structure with hydrophobic R-POSS blocks forming cores and hydrophilic poly(MPC) blocks forming shells. The aggregation number (N_{agg}) was calculated from the ratio of an apparent molecular mass of the micelle (M_w (SLS)) and the number-average molecular weight (M_n (NMR)) of the unimer (**Table 1**). The values of N_{agg} for MPC₆₁-*b*-C₂POSS₁₃, MPC₆₁-*b*-C₆POSS₁₃ and MPC₆₁-*b*-C₈POSS₁₂ were 41, 4.1 and 1.5, respectively (**Table 1**). This result suggests that aggregation ability of the copolymers decreased with increasing the long alkyl chain length of R-POSS in the copolymer. Our previous study also supported this phenomenon: the C₂H₅-POSS part in a

random copolymer of MPC and C₂H₅-POSS enhanced the hydrophobicity of a coated film interface in presence of water²⁶. It is noted that, above the CAC of MPC₆₁-*b*-C₈POSS₁₂, it aggregates with aggregation number (N_{agg}) of 1.5. Namely, it is a mixture of the polymer aggregate and unimer. In order to evaluate how the alkyl chain length affects the compaction of micelle formation, the R_g and R_h values of those copolymers were estimated (**Table 1**). The R_g values of MPC₆₁-*b*-C₂POSS₁₃, MPC₆₁-*b*-C₆POSS₁₃ and MPC₆₁-*b*-C₈POSS₁₂ were 44.9, 50.4 and 32.6, respectively. Also, the R_h values of MPC₆₁-*b*-C₂POSS₁₃, MPC₆₁-*b*-C₆POSS₁₃ and MPC₆₁-*b*-C₈POSS₁₂ were 36.1, 43.0 and 26.1, respectively. These results suggest that MPC₆₁-*b*-C₆POSS₁₃ exhibited somewhat expanded states, because both R_g and R_h values showed the highest ones although the N_{agg} value was just 4.1. Since the R_g/R_h values provide the shape of molecular aggregates, the R_g/R_h values of the copolymers were compared with each other. The R_g/R_h values of MPC₆₁-*b*-C₂POSS₁₃, MPC₆₁-*b*-C₆POSS₁₃ and MPC₆₁-*b*-C₈POSS₁₂ were 1.24, 1.17 and 1.25, respectively. It is known that the ideal R_g/R_h value of hard spherical particle is 0.778. If the packing state of the aggregates decreases or the polydispersity of the aggregates increases, then the R_g/R_h value increases around 1.5–1.7 for flexible linear chains in a good solvent³⁰. Therefore, the polymeric micelles of MPC₆₁-*b*-C₂POSS₁₃, MPC₆₁-*b*-C₆POSS₁₃ and MPC₆₁-*b*-C₈POSS₁₂ were close to a spherical shape with somewhat polydisperse in size. The polydisperse states of the micelles could be confirmed by the size distribution data obtained by DLS measurements (**Figure 1**). Since the size distribution of MPC₆₁-*b*-C₂POSS₁₃ was extremely small (**Figure 1 (A)**), MPC₆₁-*b*-C₂POSS₁₃ forms tightly packed association in conjunction with the high N_{agg} value (**Table 1**). On the other hand, MPC₆₁-*b*-C₆POSS₁₃ and MPC₆₁-*b*-C₈POSS₁₂ exhibited relatively broad two peaks representing the micelles and/or oligomers (**Figure 1 (B) and (C)**). In the case of the mixture of aggregate and unimer, SLS is analyzed as average particle information, however DLS can be analyzed separately. Considering the low N_{agg} values of MPC₆₁-*b*-C₆POSS₁₃ and MPC₆₁-*b*-C₈POSS₁₂, longer alkyl

chains of C₆H₁₃- and C₈H₁₇- on the POSS part induced loosely packed association to form the micelle. One of possible reason why the longer alkyl chains induced the loosely packed association is that the POSS modified with multi long alkyl chains is likely to form uniform micelle: Such the 7 or 8-long alkyl arms of C₈POSS stretch outward in relatively hydrophobic environment ³¹.

Transmission electron microscopy (TEM) images also supported the packing states (**Figure 2**). From the TEM images of MPC₆₁-*b*-C₂POSS₁₃, MPC₆₁-*b*-C₆POSS₁₃ and MPC₆₁-*b*-C₈POSS₁₂, spherically shaped images were observed, while they are quite polydisperse in size. Especially, TEM image of MPC₆₁-*b*-C₆POSS₁₃ (**Figure 2 (B)**) showed that the clear and monodispersed particles (diameters 30-50 nm) were uniformly distributed in a broadly distributed large aggregate. However, the size analyzed by DLS (**Figure 1 (B)**) was distributed as mentioned before. The TEM image was obtained in dry state, while the DLS data was obtained in 10 mM PBS (pH 7.4). Considering the different measuring conditions, MPC₆₁-*b*-C₆POSS₁₃ micelle was a little swollen in 10 mM PBS (pH 7.4) due to the loosely packed association, resulting in the inconsistent data between TEM and DLS. The swelling property of MPC₆₁-*b*-C₆POSS₁₃ micelle was also supported by the diameter change in water after 5 days (**Figure S3 in Supporting Information**).

ζ-Potentials of MPC₆₁-*b*-C₂POSS₁₃, MPC₆₁-*b*-C₆POSS₁₃ and MPC₆₁-*b*-C₈POSS₁₂ were -0.12, -7.5 and -0.91 mV, respectively. Only the MPC₆₁-*b*-C₆POSS₁₃ micelles showed the highest negative values. Generally, ζ-potential of PMPC in aqueous media were around 0 ~ -3 mV ^{15 32}. However, when PMPC was chemically modified on SiO₂ surfaces with 49 % surface coverage, ζ-potential of the surface was known to decrease to -5.9 mV ³³. This is presumably due to the average of the highly negative ζ-potential of SiO₂ surfaces (around -47 mV) ³⁴ and that of the PMPC. Taking the previous reports into account, the negative ζ-potential of the MPC₆₁-*b*-C₆POSS₁₃ micelles is likely due to the existence of POSS moiety near the

interface of the micelle via the loosely packed association and the polydisperse states of MPC₆₁-*b*-C₆POSS₁₃.

Table 1. Dynamic and static light scattering data each sample in 10 mM PBS (pH 7.4)

Sample	$M_w^a \times 10^5$ (g/mol)	$M_n \times 10^5$ (NMR) (g/mol)	N_{agg}^c	R_g^a (nm)	R_h^b (nm)	R_g/R_h	dn/dC_p (mL/g)	ξ -Potential (mV)	CAC ^d (DLS) (μg/ml)
MPC ₆₁ - <i>b</i> -C ₂ POSS ₁₃	10.7	0.261	41	44.9	36.1	1.24	0.0141	-0.12±0.26	49.1
MPC ₆₁ - <i>b</i> -C ₆ POSS ₁₃	1.29	0.312	4.1	50.4	43.0	1.17	0.1889	-7.5±0.60	24.5
MPC ₆₁ - <i>b</i> -C ₈ POSS ₁₂	0.497	0.325	1.5	32.6	26.1	1.25	0.1269	-0.91±0.29	91.8

^a Estimated by SLS in PBS buffer. ^b Estimated by DLS in PBS. ^c Aggregation number of a polymer micelle calculated from M_w of the micelle determined by SLS and M_w of the corresponding unimers determined by M_n (NMR). ^d Estimated by DLS measurements in deionized water.

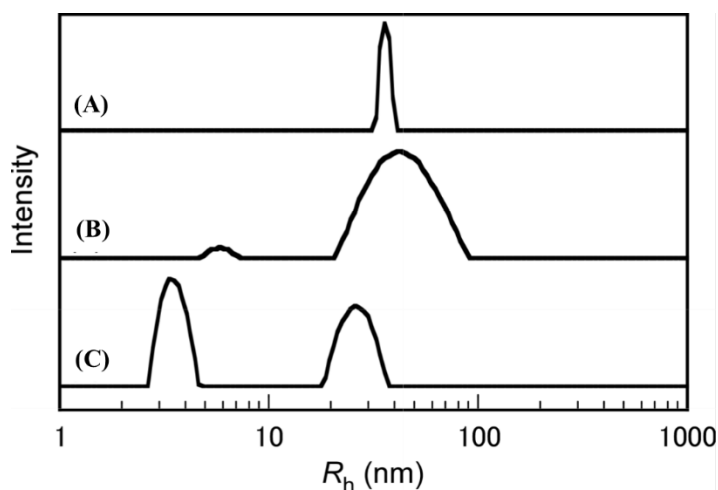


Figure 1. Intensity size distribution of (A) MPC₆₁-*b*-C₂POSS₁₃ (B) MPC₆₁-*b*-C₆POSS₁₃ and (C) and MPC₆₁-*b*-C₈POSS₁₂ in 10 mM PBS (pH 7.4).

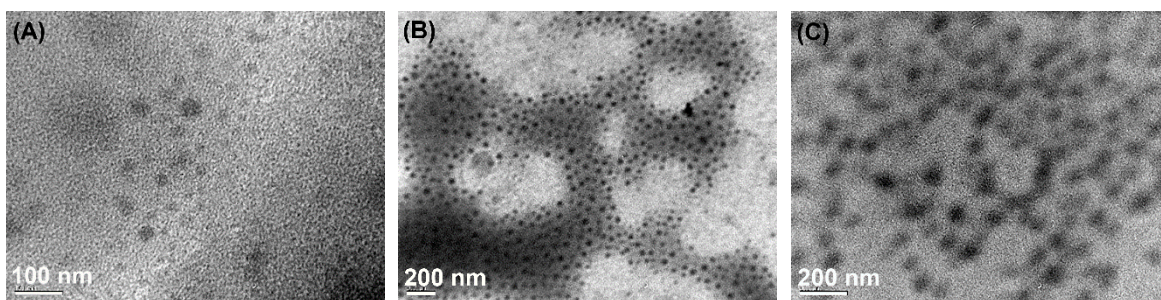


Figure 2. The TEM image of (A) MPC₆₁-*b*-C₂POSS₁₃, (B) MPC₆₁-*b*-C₆POSS₁₃ and (C) MPC₆₁-*b*-C₈POSS₁₂ in dry state (deionized water was used as solvent for micelles preparation)

The stability of the obtained micelles was determined by DLS measurements (**Figure S3 in Supporting Information**). From 0 day to 5 days, the hydrodynamic diameter of MPC₆₁-*b*-C₂POSS₁₃ decreased, indicating strong hydrophobic interaction in the core of spherical micelles and leading to shrinkage of the micelle. This shrinkage in hydrodynamic diameter suggests a tightly packed association. After standing from 5 days to 12 days at 25 °C, the hydrodynamic diameter of MPC₆₁-*b*-C₂POSS₁₃ (**Figure S3 (A)**) and MPC₆₁-*b*-C₈POSS₁₂ (**Figure S3 (C)**) did not increase. The polydispersity index (PDI) of MPC₆₁-*b*-C₂POSS₁₃ after 5 days decreased from 0.97 to 0.45 (**Table 2**) and stably maintained for 12 days. In case of the MPC₆₁-*b*-C₈POSS₁₂, even though the micelles formation was loosely packed manner but hydrophobic interaction due to the C₈H₁₇ alkyl chain maintained the micelle formation. Besides, MPC₆₁-*b*-C₆POSS₁₃ (**Figure S3 (B)**) showed growth in size after 5 days due to aggregation, suggesting that the C₆H₁₃- moiety is thermodynamically unfavourable for the micelle formation.

3.2 Characterization of drug-loaded micelles

As described in section 3.1, MPC₆₁-*b*-C₂POSS₁₃, MPC₆₁-*b*-C₆POSS₁₃ and MPC₆₁-*b*-C₈POSS₁₂ formed polymeric micelles, but the association states were governed by the R-groups of POSS moiety. In order to evaluate how the polymeric micelle formation affect poorly soluble drugs, we performed encapsulation of PTX and α -TP into the micelles.

Figure 3(a) summarized Z-average size (nm) change of polymeric micelles with or without PTX loading. **Table 2** also summarized polydispersity index (PDI) and ζ -potential (ζ) change. The diameter of MPC₆₁-*b*-C₂POSS₁₃ was found to decrease after loading of PTX (day 0), indicating the strong interaction between PTX and C₂H₅- POSS moiety, which leads to the shrinkage and well consistent with our previous data²⁷. In the case of MPC₆₁-*b*-C₈POSS₁₂, the diameter was not changed after PTX loading: the long alkyl chain (C₈H₁₇) induced the hydrophobic interaction with PTX. This phenomenon also indicates that the PTX was encapsulated in the core of the micelle. On the contrary, the hydrodynamic diameter was observed to increase for MPC₆₁-*b*-C₆POSS₁₃ micelle after PTX loading, which suggest that the large aggregation was induced by the PTX encapsulation. Considering the unstable state of MPC₆₁-*b*-C₆POSS₁₃ as seen in **Figure 1** (DLS) and **2** (TEM), the micelle-like formation was rearranged by the interaction with PTX. The PTX-loaded MPC₆₁-*b*-C₂POSS₁₃ and MPC₆₁-*b*-C₈POSS₁₂ micelles were found to be stable after 5 days at 25 °C. After 5 days, MPC₆₁-*b*-C₆POSS₁₃ showed an increase in hydrodynamic size due to the enhanced aggregation formation.

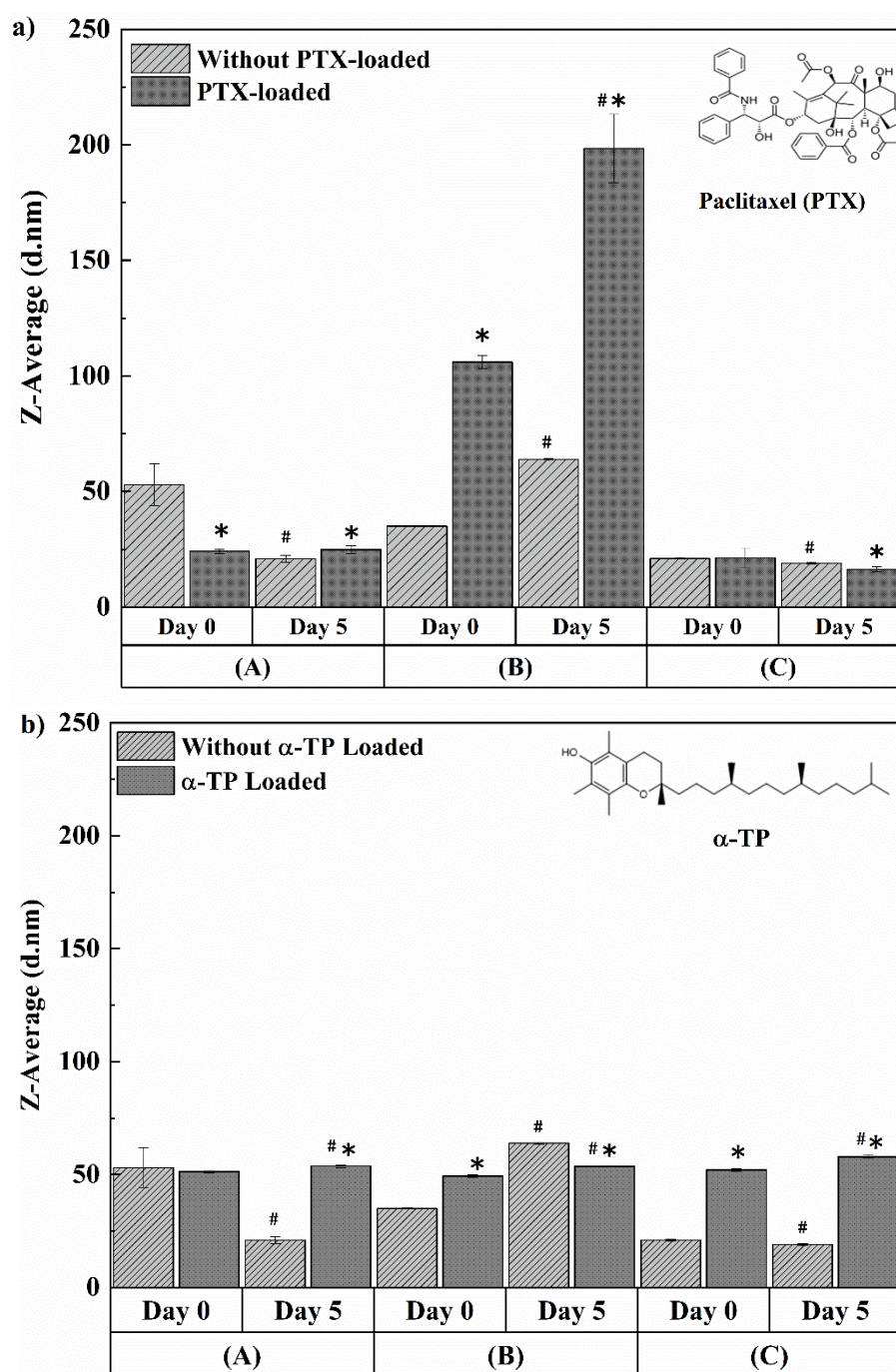


Figure 3. The stability study of copolymer (A) MPC₆₁-*b*-C₂POSS₁₃, (B) MPC₆₁-*b*-C₆POSS₁₃ and (C) MPC₆₁-*b*-C₈POSS₁₂ (n = 3); a) Z-average size (nm) change of micelles for PTX loading in deionized water b) Z-average size (nm) change of micelles for α-TP (n = 3) in deionized water at 25 °C. The concentration was 1 mg/ml. (#) indicates significantly different (p<0.05) from day 0 (Student *t*-test) and (*) indicates significantly different (p<0.05) from blank micelle (without drug loading) (Student *t*-test)

Table 2. Polydispersity Index (PDI) and ζ -Potential (ζ) of Polymeric Micelles in Deionized Water at 25 °C

Sample ^a	Without loading				PTX-loaded				α -TP-loaded			
	Day 0		Day 5		Day 0		Day 5		Day 0		Day 5	
	PDI	ζ	PDI	ζ	PDI	ζ	PDI	ζ	PDI	ζ	PDI	ζ
MPC ₆₁ - <i>b</i> -C ₂ POSS ₁₃	0.97	-0.12	0.45	-3.4	0.7	-1.8	0.86	-2.2	0.09	-23	0.1	-22
MPC ₆₁ - <i>b</i> -C ₆ POSS ₁₃	1.0	-7.5	1.0	-5.9	0.54	-9.8	0.41	-9.5	0.12	-18	0.15	-20
MPC ₆₁ - <i>b</i> -C ₈ POSS ₁₂	0.76	-0.9	0.66	-0.6	0.6	-1.8	0.6	-2.6	0.08	-20	0.15	-22

^a The concentration was 1 mg/ml.

Similar experiments were performed using α -TP (**Figure 3 b**). The diameter of all the α -TP loaded copolymers were in the range of 49-52 nm, and those were found to be stable after 5 days. Abrupt reduction of polydispersity index (PDI: 0.09 - 0.15) was observed after α -TP loading (**Table 2**), indicating the uniform size distribution. This observation indicates that α -TP molecules were encapsulated inside the micelle core, presumably due to the preferable intermolecular interaction between the aliphatic carbon chain in α -TP and the peripheral alkyl groups of POSS moiety in the micelle core and help in forming stable micelle structure³⁵.

DLC and DLE of PTX loaded micelle were calculated using Eq. (1) and (2), respectively. The DLC of PTX for MPC₆₁-*b*-C₂POSS₁₃, MPC₆₁-*b*-C₆POSS₁₃ and MPC₆₁-*b*-C₈POSS₁₂ were found to be 0.033 %, 0.024 % and 0.031 % respectively, while DLE of them were 0.44 %, 0.30 % and 0.20 %. The DLC and DLE were found to be relatively low in this case. Generally, the DLC and DLE depends not only on hydrophobicity and core size of the amphiphilic molecules but also on the chemical structure of drugs. Since PTX does not bear normal

aliphatic chains, the peripheral alkyl chains of the POSS moiety in the micelle core are not likely to fit the PTX chemical structure due to enhancement of the intermolecular interaction: the current micelle system is not suitable for high encapsulation capability of PTX . Since the POSS moieties in the polymeric micelles bears C₂-C₈ alkyl chains, the main skeleton of PTX (baccatin III) might not be fitted to the micelle core. Therefore, DLC and DLE of α -TP was alternatively investigated to gain better understanding of the phenomenon. It was observed that DLC of α -TP for MPC₆₁-*b*-C₂POSS₁₃, MPC₆₁-*b*-C₆POSS₁₃ and MPC₆₁-*b*-C₈POSS₁₂ was 3.6 %, 5.6 % and 3.6 %, respectively. Similarly, DLE of α -TP for each copolymer was 35 %, 53 % and 35 %, respectively. Since α -TP contains 4,8,12-trimethyltridecyl chain, the long aliphatic chain has the potential to provide good compatibility with aliphatic core region of the polymeric micelles via hydrophobic interactions, resulting in high DLC and DLE values. Thus, loading capacity and efficiency of the polymeric micelles were influenced by the selection of drug molecules.

3.3 *In vitro* drug release

PTX release from the MPC₆₁-*b*-C₂POSS₁₃, MPC₆₁-*b*-C₆POSS₁₃ and MPC₆₁-*b*-C₈POSS₁₂ micelles was monitored by a dialysis method for 52 h. In order to approximate an infinite sink without requiring simulated flow conditions, the addition of surfactants such as Tween 80²⁹ and *N,N*-diethylnicotinamide³⁶ to the release medium is general protocols. Here, 1 % Tween 80 was used as surfactant to solubilize PTX for maintaining the sink condition for accurate measurements. However, the PTX concentration in the outer medium at each sampling time could not be determined because the PTX concentration in the outer medium was below the detection limit of the HPLC measurements. This indicates the strong interaction between PTX and micelle inside the core, which leads to negligible level of PTX release from the micelles. Additionally, α -TP release was also investigated to compare the PTX release (**Figure 4**). It was

found that even after 61 h, the α -TP release from MPC₆₁-*b*-C₂POSS₁₃, MPC₆₁-*b*-C₆POSS₁₃ and MPC₆₁-*b*-C₈POSS₁₂ micelles was 37 %, 12 % and 20 %, respectively. Because of higher DLC and DLE of α -TP than those of PTX, the detectable amount of α -TP released slowly to the outer medium was determined. Both the phenomena can be explained that, once the drugs were encapsulated to the micelle core, most of the drugs were maintained in the micelles.

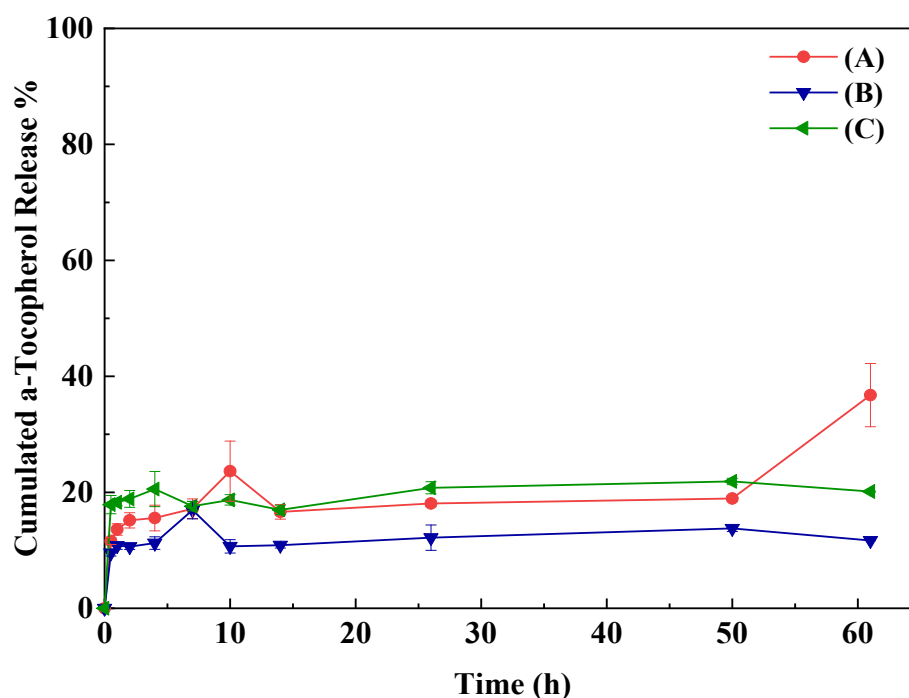


Figure 4. α -TP release from α -TP -loaded micelles: vs. time curves (A) MPC₆₁-*b*-C₂POSS₁₃, (B) MPC₆₁-*b*-C₆POSS₁₃ and (C) MPC₆₁-*b*-C₈POSS₁₂ micelles. Values are mean \pm S.D. (n = 3).

3.4 Cell viability

Cell viability of the copolymers were evaluated using HeLa cells. All the copolymers showed excellent cell viability after 24 and 48 h (**Figure S4 in Supporting Information**). The cytotoxic activity of PTX-loaded polymeric micelles was evaluated (initial PTX concentration: 2 μ g/ml) (**Figure 5**). After 24 h, the cell viability was almost 90 % in all the PTX-loaded copolymers and free PTX. After 48 h, the cell viability reduced to around 50 % in all the

copolymers and PTX. This means that, if the efficacy of cellular uptake of the copolymers was assumed to be similar to the free PTX, those copolymers can release PTX in the intracellular environments rapidly, or the PTX-loaded micelles themselves acted as the anticancer compounds. Xu *et al* reported that HeLa cell viability of free PTX at 10 $\mu\text{g/ml}$ was about 50 and 30 %, for 24 and 48 h of incubation respectively³⁷. In our case, PTX concentration was 2 $\mu\text{g/ml}$, which is much less than the reported concentration to decrease the cell viability after 24 h. This is why it took 48 h to decrease the cell viability. However, it is difficult to understand why there were no difference between the free PTX and the PTX-loaded micelles, and therefore, cellular uptake study was performed.

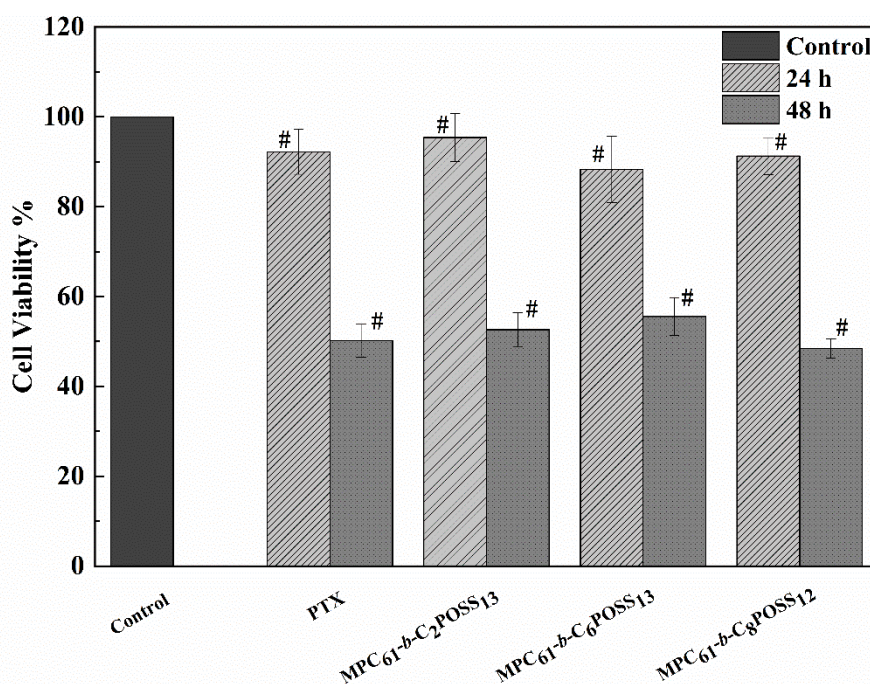


Figure 5. The cell viability % in presence of PTX-loaded copolymer micelle: MPC₆₁-b-C₂POSS₁₃, MPC₆₁-b-C₆POSS₁₃ and MPC₆₁-b-C₈POSS₁₂ (each micelle contains PTX concentration 2 $\mu\text{g/ml}$ seeded cell plate). Each of the solutions (10 μl) were added to HeLa cells seeded well plate (90 μl) and incubated for 24 h and 48 h at 37 °C to measure the cell viability. Values are mean \pm S.D. (n = 6). Cell viability was determined using the CCK-8 Kits and the absorbance was detected at 450 nm. (#) indicate significantly different ($p < 0.05$) from control sample (Two sample *t*-test).

3.5 Cellular uptake

Cellular uptake of the copolymers and its intracellular localization were investigated by using FITC-PTX-loaded copolymer^{27, 38}. FITC-PTX (**Figure S5 in Supporting Information**) was used as a green fluorescent probe, and the green fluorescent intensity was considered to be attributed by the FITC-PTX that was loaded in the copolymer micelles. **Figure 6** shows the fluorescent microscope images of HeLa cells after 2 h incubation with free FITC-PTX and FITC-PTX-loaded micelles. The fluorescent intensity of free FITC-PTX in the cells is likely to increase as compared to control. Similarly, the green fluorescent color of the FITC-PTX-loaded MPC₆₁-*b*-C₂POSS₁₃ and MPC₆₁-*b*-C₆POSS₁₃ was found inside the cells after 2 h. It is to note that the intensity of FITC-PTX-loaded MPC₆₁-*b*-C₈POSS₁₂ seemed to be enhanced as compared with the other two copolymers. The fluorescent intensity of FITC-PTX in the cells increased with incubation time (6 h) (**Figure S6 in Supporting Information**). These results suggest that the MPC₆₁-*b*-C₈POSS₁₂ might modulate the cellular uptake. However, since this hypothesis is just based on the qualitative observation, we conducted FACS measurements of the same sample series for 2 h incubation.

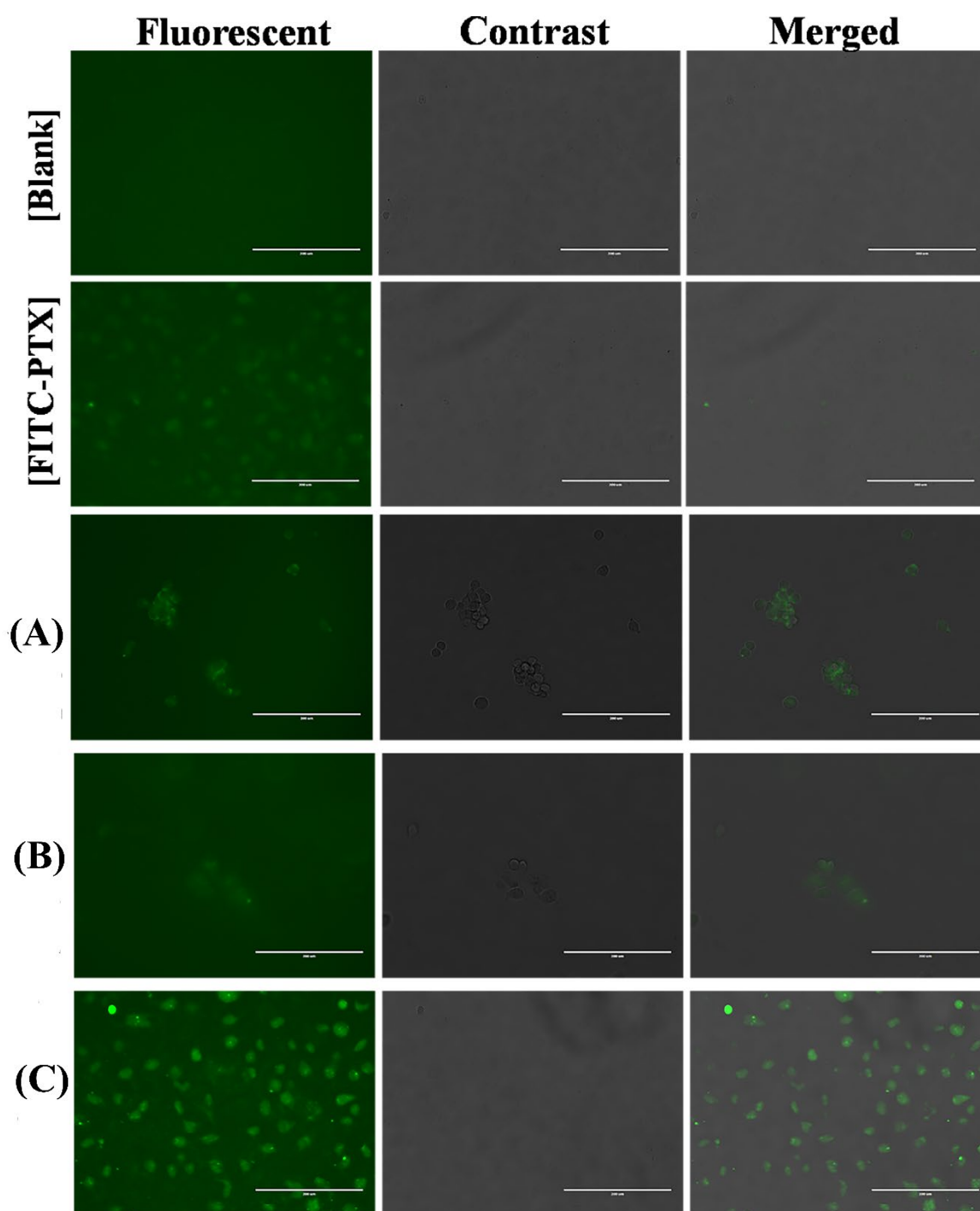


Figure 6. Fluorescence microscopy images of HeLa cells treated with medium only (control), free FITC-PTX, (A) MPC₆₁-*b*-C₂POSS₁₃, (B) MPC₆₁-*b*-C₆POSS₁₃ and (C) MPC₆₁-*b*-C₈POSS₁₂ (each micelle contains paclitaxel concentration 2 µg/ml seeded cell plate) after 2 h incubation. Scale bar: 200 µm

3.6 Quantitative assessment of cellular uptake: Flow cytometry

The flow cytometry results were summarized in **Figure 7**. As shown in **Figure 7(a)**, both the free FITC-PTX and the FITC-PTX-loaded copolymers increased the intensity level as compared to control, indicating the cellular uptake of both the free FITC-PTX and the FITC-PTX-loaded copolymers for 2h. In order to quantitatively discuss the cellular uptake, mean fluorescence intensity (MFI) was calculated and summarized in **Figure 7(b)**. The MFI of the FITC-PTX-loaded MPC₆₁-*b*-C₆POSS₁₃ and MPC₆₁-*b*-C₈POSS₁₂ micelles were found to be no different from free FITC-PTX, while only the MFI of FITC-PTX-loaded MPC₆₁-*b*-C₂POSS₁₃ micelle was significantly smaller than that of the free FITC-PTX. Considering the tightly packed association state of MPC₆₁-*b*-C₂POSS₁₃ micelle (**Table. 1** and **Figure 1**), it can be considered that the relatively harder morphology of MPC₆₁-*b*-C₂POSS₁₃ micelle might reduce the cellular uptake. Among the copolymer micelles, the cellular uptake of the FITC-PTX-loaded MPC₆₁-*b*-C₆POSS₁₃ was higher than that of the MPC₆₁-*b*-C₂POSS₁₃ and MPC₆₁-*b*-C₈POSS₁₂. Previous reports suggest that the particle size and the distribution play an important role in cellular uptake which achieves a maximum in the size range of ~25-35 nm. Cellular uptake goes down for larger particles. The cellular uptake also depends on the surface charge (negative zeta potential caused electrostatic repulsion and hamper particle membrane interaction), hydrophobic nature of the core of the particle. It is noted that the size of PTX-loaded MPC₆₁-*b*-C₆POSS₁₃ was around 106 nm (see **Figure 3 a**): higher than the other copolymers), and the zeta potential was -10 mV (the highest negative charge among the copolymers) after PTX loading (**Table 2**). Taking the unstable micelle formation of MPC₆₁-*b*-C₆POSS₁₃ into account (**Figure 3 a**), the amphiphilic unimer or oligomers of MPC₆₁-*b*-C₆POSS₁₃ might disrupt cellular membrane to enhance the uptake. Overall, cellular uptake level of the FITC-PTX-loaded micelles was similar to the free FITC-PTX, suggesting the PMPC shell of the micelles did not disturb the cellular uptake. Recently, de Castro *et al.* and

Li *et al.* reported that PMPC have a strong affinity towards specific receptors that are expressed by most of the cells due to the phosphorylcholine group^{32, 18}. Therefore, the PMPC shells of the copolymers are likely to enhance the uptake similar to the free FITC-PTX, although the mechanism of uptake was independent. Thus, PTX-loaded MPC₆₁-*b*-C₆POSS₁₃ enhanced the uptake, but the cell viability was almost same as the other micelles (**Figure 5**). Although the loosely packed association of MPC₆₁-*b*-C₆POSS₁₃ enable to disrupt cellular membrane as mentioned above, the very slow release of PTX during 48 h dominated the cell viability.

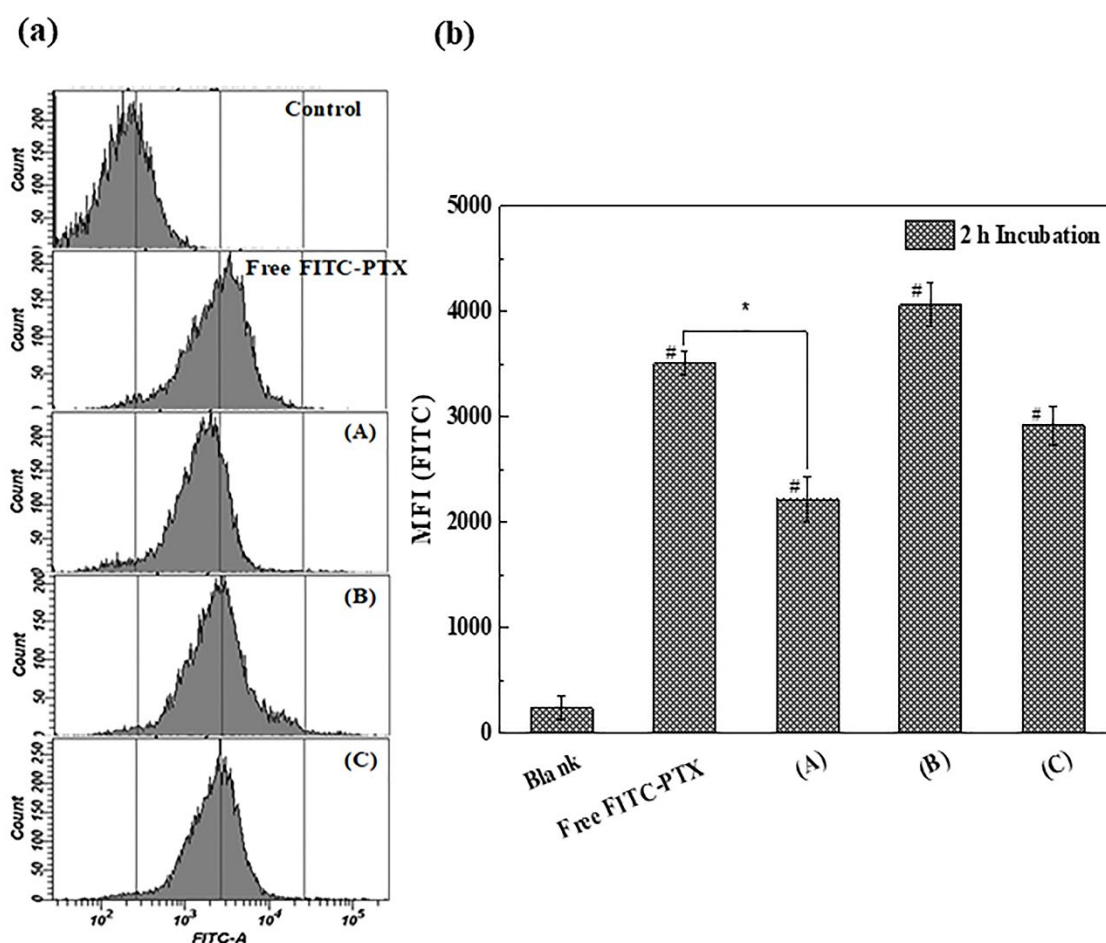


Figure 7. Flow cytometry data of (a) histograms (count vs fluorescence intensity) and (b) the mean fluorescent intensity for FITC-PTX-loaded copolymer micelles (A) MPC₆₁-*b*-C₂POSS₁₃, (B) MPC₆₁-*b*-C₆POSS₁₃ and (C) MPC₆₁-*b*-C₈POSS₁₂ (each micelle contains FITC-PTX concentration 2 µg/ml seeded cell plate) in HeLa cells after 2 h incubation. The mean fluorescence intensity was calculated by total 10000 events. (*) Statistically significantly

difference compared to free FITC-PTX and (#) statistically significantly difference compared to control.

4. Conclusion

In this study, amphiphilic di-block copolymers of 2-(methacryloyloxy)ethyl phosphorylcholine (MPC) and methacrylate R-POSS (vertex R-groups of POSS cage modified with ethyl (C_2H_5), hexyl (C_6H_{13}), octyl (C_8H_{17}) alkyl chain) were synthesized via RAFT polymerization. All the di-block copolymers formed spherical micelles in an aqueous environment within the range of 26-43 nm. By changing the alkyl chain length of R-POSS block, solution properties of the polymeric micelles were modulated: C_2H_5 induced tightly packed association, in which ca. 41 $MPC_{61}-b-C_2POSS_{13}$ molecules were associated. By changing the R-groups to C_6H_{13} and C_8H_{17} , they induced loosely packed association, in which ca. 2-4 di-block copolymer molecules were associated. We found that only $MPC_{61}-b-C_6POSS_{13}$ micelle was unstable due to the polydisperse nature. All the micelles were able to encapsulate hydrophobic drugs inside the core, the stability of which was dependent on the chemical structure of the drugs: poorly soluble drugs bearing long alkyl chains such as α -TP were suitable for the R-POSS core. Cellular uptake of PTX-loaded micelles was governed by the PMPC-related cellular uptake phenomena. Therefore, the amphiphilic copolymers of MPC and R-POSS prepared by RAFT polymerization could be a promising candidate for controlled micelle formation and the selective hydrophobic drug encapsulation and potential as a carrier for drug delivery.

Supporting Information.

- Characterization of di-block copolymers (1H NMR and FT-IR spectra of $MPC_{61}-b-C_2POSS_{13}$, $MPC_{61}-b-C_6POSS_{13}$ and $MPC_{61}-b-C_8POSS_{12}$); Particle size (Z-average

diameter) change of the micelles in water during 12 days. ; The cell viability of the copolymers; Chemical structure of FITC-PTX; Fluorescence microscopy images of HeLa cells treated with free FITC-PTX and the FITC-PTX-contained micelles.

Acknowledgments:

This study was financially supported from a Grant-in-Aid for Scientific Research on Innovative Areas “New Polymeric Materials Based on Element-Blocks (No.2401)” (JSPS KAKENHI grant number JP15H00748) and Izumi Science and Technology Foundation, Japan (2018-J-75). The authors also thank Toshimi Otsuka Scholarship Foundation for supporting the international student during this work.

References

1. Luo, S.; Zhang, Y. X.; Cao, J.; He, B.; Li, S., Arginine modified polymeric micelles as a novel drug delivery system with enhanced endocytosis efficiency. *Colloid Surface B* **2016**, 148, 181-192.
2. Xu, J. P.; Ji, J.; Chen, W. D.; Shen, J. C., Novel biomimetic polymersomes as polymer therapeutics for drug delivery. *J Control Release* **2005**, 107, (3), 502-512.
3. Siegwart, D. J.; Oh, J. K.; Matyjaszewski, K., ATRP in the design of functional materials for biomedical applications. *Prog Polym Sci* **2012**, 37, (1), 18-37.
4. Zhou, J. H.; Wang, L.; Ma, J. Z., Recent Research Progress in the Synthesis and Properties of Amphiphilic Block Co-polymers and Their Applications in Emulsion Polymerization. *Des Monomers Polym* **2009**, 12, (1), 19-41.
5. Zhang, H. Q., Controlled/"living" radical precipitation polymerization: A versatile polymerization technique for advanced functional polymers. *Eur Polym J* **2013**, 49, (3), 579-600.

6. Charleux, B.; Delaittre, G.; Rieger, J.; D'Agosto, F., Polymerization-Induced Self-Assembly: From Soluble Macromolecules to Block Copolymer Nano-Objects in One Step. *Macromolecules* **2012**, 45, (17), 6753-6765.
7. Chiefari, J.; Chong, Y. K.; Ercole, F.; Krstina, J.; Jeffery, J.; Le, T. P. T.; Mayadunne, R. T. A.; Meijs, G. F.; Moad, C. L.; Moad, G.; Rizzardo, E.; Thang, S. H., Living free-radical polymerization by reversible addition-fragmentation chain transfer: The RAFT process. *Macromolecules* **1998**, 31, (16), 5559-5562.
8. Moad, G.; Rizzardo, E.; Thang, S. H., Living radical polymerization by the RAFT process - A first update. *Aust J Chem* **2006**, 59, (10), 669-692.
9. Moad, G.; Rizzardo, E.; Thang, S. H., Living Radical Polymerization by the RAFT Process - A Second Update. *Aust J Chem* **2009**, 62, (11), 1402-1472.
10. Moad, G.; Rizzardo, E.; Thang, S. H., Living Radical Polymerization by the RAFT Process - A Third Update. *Aust J Chem* **2012**, 65, (8), 985-1076.
11. Fairbanks, B. D.; Gunatillake, P. A.; Meagher, L., Biomedical applications of polymers derived by reversible addition - fragmentation chain-transfer (RAFT). *Adv Drug Deliver Rev* **2015**, 91, 141-152.
12. Qian, W. H.; Song, X. M.; Feng, C.; Xu, P. C.; Jiang, X.; Li, Y. J.; Huang, X. Y., Construction of PEG-based amphiphilic brush polymers bearing hydrophobic poly(lactic acid) side chains via successive RAFT polymerization and ROP. *Polym Chem-Uk* **2016**, 7, (19), 3300-3310.
13. Stenzel, M. H.; Barner-Kowollik, C.; Davis, T. P.; Dalton, H. M., Amphiphilic block copolymers based on poly (2-acryloyloxyethyl phosphorylcholine) prepared via RAFT polymerisation as biocompatible nanocontainers. *Macromol Biosci* **2004**, 4, (4), 445-453.
14. Yusa, S. I.; Fukuda, K.; Yamamoto, T.; Ishihara, K.; Morishima, Y., Synthesis of well-defined amphiphilic block copolymers having phospholipid polymer sequences as a novel biocompatible polymer micelle reagent. *Biomacromolecules* **2005**, 6, (2), 663-670.

15. Konno, T.; Kurita, K.; Iwasaki, Y.; Nakabayashi, N.; Ishihara, K., Preparation of nanoparticles composed with bioinspired 2-methacryloyloxyethyl phosphorylcholine polymer. *Biomaterials* **2001**, 22, (13), 1883-1889.
16. Pegoraro, C.; Cecchin, D.; Gracia, L. S.; Warren, N.; Madsen, J.; Armes, S. P.; Lewis, A.; MacNeil, S.; Battaglia, G., Enhanced drug delivery to melanoma cells using PMPC-PDPA polymersomes. *Cancer Lett* **2013**, 334, (2), 328-337.
17. Colley, H. E.; Hearnden, V.; Avila-Olias, M.; Cecchin, D.; Canton, I.; Madsen, J.; MacNeil, S.; Warren, N.; Hu, K.; McKeating, J. A.; Armes, S. P.; Murdoch, C.; Thornhill, M. H.; Battaglia, G., Polymersome-Mediated Delivery of Combination Anticancer Therapy to Head and Neck Cancer Cells: 2D and 3D in Vitro Evaluation. *Mol Pharmaceut* **2014**, 11, (4), 1176-1188.
18. Li, L.; Song, Y.; He, J. L.; Zhang, M. Z.; Liu, J.; Ni, P. H., Zwitterionic shielded polymeric prodrug with folate-targeting and pH responsiveness for drug delivery. *J Mater Chem B* **2019**, 7, (5), 786-795.
19. Ayandele, E.; Sarkar, B.; Alexandridis, P., Polyhedral Oligomeric Silsesquioxane (POSS)-Containing Polymer Nanocomposites. *Nanomaterials-Basel* **2012**, 2, (4), 445-475.
20. Hussain, H.; Tan, B. H.; Seah, G. L.; Liu, Y.; He, C. B.; Davis, T. P., Micelle Formation and Gelation of (PEG P(MA-POSS)) Amphiphilic Block Copolymers via Associative Hydrophobic Effects. *Langmuir* **2010**, 26, (14), 11763-11773.
21. Tan, B. H.; Hussain, H.; He, C. B., Tailoring Micelle Formation and Gelation in (PEG-P(MA-POSS)) Amphiphilic Hybrid Block Copolymers. *Macromolecules* **2011**, 44, (3), 622-631.
22. Zhang, Z. H.; Xue, Y. D.; Zhang, P. C.; Muller, A. H. E.; Zhang, W. A., Hollow Polymeric Capsules from POSS-Based Block Copolymer for Photodynamic Therapy. *Macromolecules* **2016**, 49, (22), 8440-8448.
23. Fan, L. F.; Wang, X.; Cao, Q. C.; Yang, Y. Y.; Wu, D. C., POSS-based supramolecular amphiphilic zwitterionic complexes for drug delivery. *Biomater Sci-Uk* **2019**, 7, (5), 1984-1994.

24. Yuan, H.; Luo, K.; Lai, Y. S.; Pu, Y. J.; He, B.; Wang, G.; Wu, Y.; Gu, Z. W., A Novel Poly(L-glutamic acid) Dendrimer Based Drug Delivery System with Both pH-Sensitive and Targeting Functions. *Mol Pharmaceut* **2010**, 7, (4), 953-962.
25. Fan, X. S.; Hu, Z. G.; Wang, G. W., Synthesis and unimolecular micelles of amphiphilic copolymer with dendritic poly(L-lactide) core and poly(ethylene oxide) shell for drug delivery. *Rsc Adv* **2015**, 5, (122), 100816-100823.
26. Chatterjee, S.; Matsumoto, T.; Nishino, T.; Ooya, T., Tuned Surface and Mechanical Properties of Polymeric Film Prepared by Random Copolymers Consisting of Methacrylate-POSS and 2-(Methacryloyloxy)ethyl Phosphorylcholine. *Macromol Chem Phys* **2018**, 219, (8), 1700572.
27. Chatterjee, S.; Ooya, T., Hydrophobic Nature of Methacrylate-POSS in Combination with 2-(Methacryloyloxy)ethyl Phosphorylcholine for Enhanced Solubility and Controlled Release of Paclitaxel. *Langmuir* **2018**, 35, (5), 1404-1412.
28. Chatterjee, S.; Ooya, T., Amphiphilic Copolymer of Polyhedral Oligomeric Silsesquioxane (POSS) Methacrylate for Solid Dispersion of Paclitaxel. *Materials (Basel)* **2019**, 12, (7), 1058.
29. Yang, T.; Cui, F. D.; Choi, M. K.; Cho, J. W.; Chung, S. J.; Shim, C. K.; Kim, D. D., Enhanced solubility and stability of PEGylated liposomal paclitaxel: In vitro and in vivo evaluation. *Int J Pharmaceut* **2007**, 338, (1-2), 317-326.
30. Huber, K.; Bantle, S.; Lutz, P.; Burchard, W., Hydrodynamic and Thermodynamic Behavior of Short-Chain Polystyrene in Toluene and Cyclohexane at 34.5-Degrees-C. *Macromolecules* **1985**, 18, (7), 1461-1467.
31. Han, J.; Zheng, Y. C.; Zheng, S.; Li, S. P.; Hu, T. N.; Tang, A. J.; Gao, C., Water soluble octa-functionalized POSS: all-click chemistry synthesis and efficient host guest encapsulation. *Chem Commun* **2014**, 50, (63), 8712-8714.
32. de Castro, C. E.; Ribeiro, C. A. S.; Alavarse, A. C.; Albuquerque, L. J. C.; da Silva, M. C. C.; Jager, E.; Surman, F.; Schmidt, V.; Giacomelli, C.; Giacomelli, F. C., Nanoparticle-Cell Interactions: Surface Chemistry Effects on the Cellular Uptake of Biocompatible Block Copolymer Assemblies. *Langmuir* **2018**, 34, (5), 2180-2188.

33. Sakata, S.; Inoue, Y.; Ishihara, K., Quantitative Evaluation of Interaction Force between Functional Groups in Protein and Polymer Brush Surfaces. *Langmuir* **2014**, 30, (10), 2745-2751.
34. Xu, Y.; Takai, M.; Ishihara, K., Protein adsorption and cell adhesion on cationic, neutral, and anionic 2-methacryloyloxyethyl phosphorylcholine copolymer surfaces. *Biomaterials* **2009**, 30, (28), 4930-4938.
35. Tao, L.; Chan, J. W.; Uhrich, K. E., Drug loading and release kinetics in polymeric micelles: Comparing dynamic versus unimolecular sugar-based micelles for controlled release. *J Bioact Compat Pol* **2016**, 31, (3), 227-241.
36. Ooya, T.; Lee, J.; Park, K., Effects of ethylene glycol-based graft, star-shaped, and dendritic polymers on solubilization and controlled release of paclitaxel. *J Control Release* **2003**, 93, (2), 121-127.
37. Xu, Q.; Liu, Y. X.; Su, S. S.; Li, W.; Chen, C. Y.; Wu, Y., Anti-tumor activity of paclitaxel through dual-targeting carrier of cyclic RGD and transferrin conjugated hyperbranched copolymer nanoparticles. *Biomaterials* **2012**, 33, (5), 1627-1639.
38. Gong, C. Y.; Xie, Y. M.; Wu, Q. J.; Wang, Y. J.; Deng, S. Y.; Xiong, D. K.; Liu, L.; Xiang, M. L.; Qian, Z. Y.; Wei, Y. Q., Improving anti-tumor activity with polymeric micelles entrapping paclitaxel in pulmonary carcinoma. *Nanoscale* **2012**, 4, (19), 6004-6017.

Table of Contents (TOC) graphic

